XVI IMEKO World Congress
Measurement - Supports Science - Improves Technology - Protects Environment ... and Provides Employment - Now and in the Future
Vienna, AUSTRIA, 2000, September 25-28

PANORAMIC INTERFEROMETRY OF CYLINDRICAL SHELLS

E.A. Krasnopevtsev and L.A. Borynyak
Department of Physics, State Pedagogical University
Novosibirsk, Siberia, Russian Federation

Abstract: A panoramic holographic interferometer with the maximum angle aperture is proposed. The main element is a conic mirror with an apex angle 90° and coaxial with the cylindrical object. Near the object a cylindrical photoemulsion film is placed. Peculiarities of image and of interference picture restored by an unrolled two-exposured hologram are examined. Measurement methods of all displacement vector components of the external and internal surface points of the optically transparent shell are expounded. Sensitivity is equal in all surface points. Tomographical measurement methods of relative radial deformation of the shell elements are elaborated. The unrolled hologram creates a wall shell image like a flat layer. Radon transformation of a flat layer and reconstruction of a low frequency deformed state on the basis of a 2D summary images are considered. Unrolled hologram allows to determine an object-deformed state in separate points and also as a whole and expose anomalous deformation zones.

Keywords: interferometry, panoramic, holographic

1 INTRODUCTION

Panoramic interferometers [1] study deformed state of cylindrical objects with diameter of (5 ÷ 100) mm, using ray beams with axial symmetry. The proposed panoramic interferometer has a conical mirror with an apex angle 90° and coaxial with an object. A photoemulsion has the form of cylindrical shell, and is placed near the surface under study, therefore the maximal aperture is achieved. The axial collimated coherent beam falls on the conical mirror. After two exposures the hologram is unrolled in plate and set of panoramic interferograms in collimated beams is created. This panoramic interferometer with cylindrical hologram measures the whole displacement vector with equal sensitivity for all points of the surface within the range of (0.3 – 50)λ. As optical tomograph this interferometer investigates the deformed state of optically transparent wall of the shell.

2 IMAGE RECONSTRUCTION BY UNROLLED HOLOGRAM

The panoramic interferometer in figure 1 creates a cylindrical illuminating and reference wave. An object surface scatters the radiation and waves pass through the photoemulsion *H* located on cylindrical glass tube. In figure 2a the axial cross-section geometry of the interferometer is

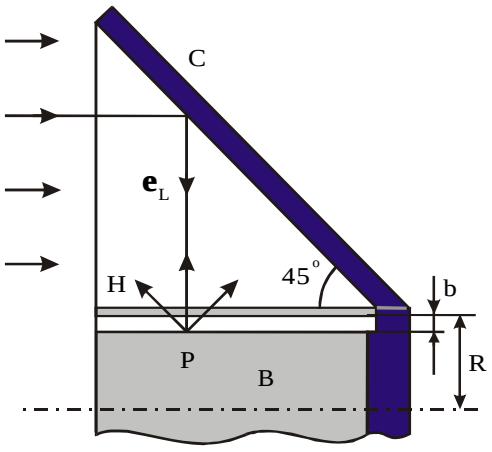

Figure 1. Panoramic interferometer with cylindrical hologram: *C* - conical mirror, *H* - photoemulsion on cylindrical glass tube, *B* - object.

represented. The reference wave and an object's point *B* wave produce the interference maximums. If the process of image reconstruction is considered, then interference maximums will be treated as a system of small mirrors. While unrolling the hologram the position of such mirrors, their orientation, and the distance between them change. Small interference mirrors *Ð*$_{\hat{i}}$-*Ð*$_{\hat{i}}$ and *Ð*-*Ð* in figure 2 are within the neutral layer *M*-*M*. The process of image reconstruction upon unrolling the hologram and illuminating by the normal collimated reference beam is shown in figure 2b. The point *B'* is an image of point *B*. Since upon bending the hologram the axial cross sections remain plane, then the angle between the line *M*-*M* and the normal *N*-*N* does not change. The radial distance *b* is reckoned along the radius from the line *M*-*M* to the point *B*. From figure 2 it follows: $\beta_1 = 2\theta = \beta - \alpha$, $t = [b - R \cdot (1 - \cos\alpha)] \cdot tg\,\beta = R \cdot \sin\alpha$, $t_1 = b_1 \cdot tg(2\theta) = R \cdot \alpha$. For $b << R$ we obtain $\alpha = (b \cdot tg\,\beta)/R$, then $b_1 = \hat{a} - \frac{b}{R} \cdot tg\hat{a}$ and for $\beta \le 45°$ we have $\alpha << 1$. Expanding the previous expressions into series with respect to α we find $b_1 = b + \Delta b$. To within the first power (b/R) the value of Δb has the form $\Delta b = \frac{b^2}{R} \cdot (1 + \frac{1}{2} tg^2 b)$ and

$$b_1 = b \cdot [1 + \frac{b}{R} \cdot (1 + \frac{1}{2} tg^2 b)] . \qquad (1)$$

To decrease the radial distortion we must place the photoemulsion as close to the object as possible, and decrease the observation angle β.

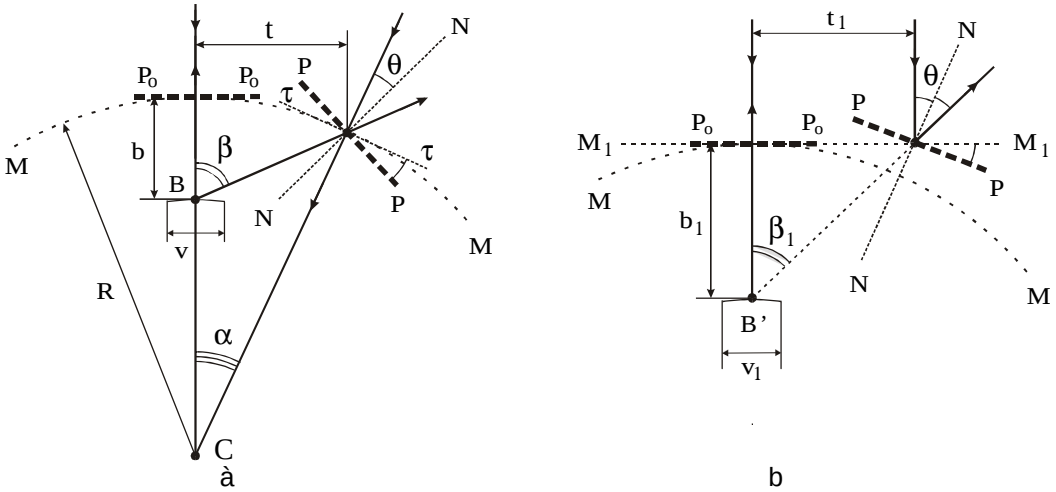

Figure 2. Position of the interference mirrors *Ð*$_{\hat{i}}$-*Ð*$_{\hat{i}}$ and *Ð*-*Ð* before unrolling the hologram (a) and after (b): *B* is an object point, *B*' is the object point image, *C* is the curvature center of the line *M*-*M*.

The image tangential size v in figure 2 changes while unrolling the hologram. We will consider two points on the cylindrical object surface spaced at a distance v, and $v << R$. The radial lines from the point *C* on the interferometer axis to these points make the angle $\gamma = v/(R - b)$. Upon unrolling the hologram these lines remain "frozen" in it. The images of the points, remaining on these lines, move away from each other by $\Delta v = \gamma \cdot b_1 = v \cdot b \cdot \{1 + (b/R) \cdot [1 + (tg^2\beta)/2]\}/(R - b)$, and the distance between the points becomes equal to $v_1 = v + \Delta v$. To within the first power (b/R) the value of v has the form

$$v = v_1 \cdot (1 - \frac{b}{R}) . \qquad (2)$$

For example, for R = 20 mm, b = 3 mm, $\beta = 45°$ from formulas (1), (2) we obtain $\Delta b = 0.7$ mm, $\Delta v/v = 0.21$.

To estimate the aberration introduced by the change in the distances between the interference maximums upon bending the hologram, we will represent it in the form of thin layers, each layer being a reflective diffractive grating. The calculation shows that we can neglect the change in the image position if *l* << b, which takes place practically everywhere. The microscopic changes in the distances between the interference maximums result in scattering of reflected beams and in appearance of speckles.

If the cylindrical surface is observed in parallel rays lying in the plane perpendicular to axis, then all its points receive equal radial displacements. An image formed by beams lying in the axial plane of a cylindrical hologram is reconstructed upon its bending without distortions.

The relationship between the initial interference pattern and the pattern obtained by unrolling the hologram is determined by the initial displacement vector components (u, v, and w) and the "unrolled" ones (u_1, v_1, and w_1). The axial component u is not changed, the tangential component v is transformed according to (2), and the radial component w is not distorted if it is viewed in the axial plane and transformed in the same manner as the differential of the value *b* in expression (1) while viewing in the plane perpendicular to the axis. As a result, accurate within *b/R* we obtain

$$u_1 = u, \quad v = v_1 \cdot (1 - \frac{b}{R}), \quad w_{1\parallel} = w, \quad w_{1\perp} = w \cdot [1 + \frac{2b}{R} \cdot (1 + \frac{1}{2} tg^2 b_1)]. \tag{3}$$

3 MEASUREMENT OF THE DISPLACEMENT VECTOR COMPONENTS OF SURFACE POINTS

Normal illumination of the plane of the two-exposure hologram by a collimated reference beam reconstructs both object states and they are observed and interfere in parallel beams of different directions. To measure the components (u_1, v_1, w_1) we must fix three panoramic interferograms. Let us specify the beam directions by means of the angular parameters β_1 and γ (figure 3). The relationship

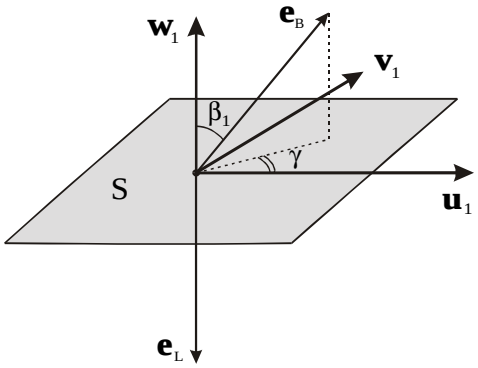

Figure 3. Position of the components $\mathbf{u}_1$, $\mathbf{v}_1$, $\mathbf{w}_1$ of the displacement vector in the surface point S.

between the absolute order $m(\beta_1,\gamma)$ of the interference fringe at some point and the displacement vector $\mathbf{D}_1(u_1,v_1,w_1)$ for it has the form [2]: $(\mathbf{e}_B - \mathbf{e}_L)\,\mathbf{D}_1 = m\,\lambda$, $\mathbf{e}_B$ and $\mathbf{e}_L$ are the unit vectors of view and illumination. Using the parameters of figure 3, this equation can be written in the form

$$w_1 \cdot (1 + \cos\beta_1) + u_1 \cdot \sin\beta_1 \cdot \cos\gamma + v_1 \cdot \sin\beta_1 \cdot \sin\gamma = \lambda \cdot m(\beta_1,\gamma). \tag{4}$$

Changing continuously the view vector direction over a wide range of angles, we can follow the shift of the fringes over the shell surface, the number of each fringe is preserved, and we can coordinate the numbers of fringes on different interferograms.

Let us find the value w by choosing for viewing the axial plane of the interferometer with the angles $\gamma = 0$, $\beta_1 = \varepsilon$ ($\varepsilon << 1$). The condition $\varepsilon \neq 0$ is necessary for eliminating the light spot from the reference beam. From (3) and (4) we obtain

$$w = \frac{l}{2} \cdot m(e,0). \tag{5}$$

For illustration, figure 4 represents an interferogram obtained by an unrolled hologram with $\gamma = 0$,

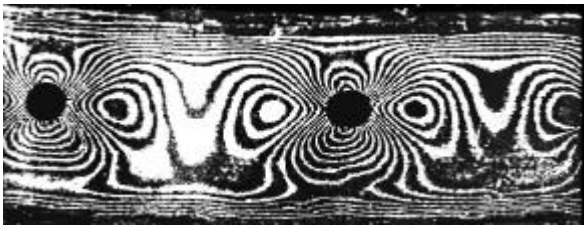

Figure 4. An unrolled panoramic interferogram.

$\beta_1 = \varepsilon$. The object was a cylindrical shell with two symmetric circular cuts, which was pressed by the axial force.

Choosing for observation the axial plane of the interferometer $\gamma = 0$ and the angle $\beta_1 \neq 0$, we find from (3) – (5)

$$u = \frac{l}{\sin b_1} \cdot \left[m(b_1,0) - \frac{1+\cos b_1}{2} \cdot m(e,0) \right]. \tag{6}$$

Choosing the view plane perpendicular to the interferometer axis, i.e., with the angles $\gamma = 90°$, $\beta_1 \neq 0$, we obtain from (3) – (5)

$$v = \frac{l}{\sin b_1} \cdot \left[(1 - \frac{b}{R}) \cdot m(b_1,90°) - \frac{1+\cos b_1}{2} \cdot (1 + \frac{b}{R} \cdot \frac{1}{\cos^2 b_1}) \cdot m(e,0) \right]. \tag{7}$$

The coefficient connecting the values u, v, and w to m in formulas (5) – (7) are independent of the position of the point on the surface, that is why the measurement sensitivity of each component of the displacement vector is the same for all points of the surface.

4 MEASUREMENT OF RADIAL DEFORMATION OF ELEMENTS OF A SHELL WALL

The panoramic interferometer with cylindrical hologram in figure 5 is intended for investigation of the deformed state of the volume-elements of a transparent cylindrical shell. The collimated coherent ray beam *A*, upon reflecting from the conic mirror *C*, passes through the cylindrical

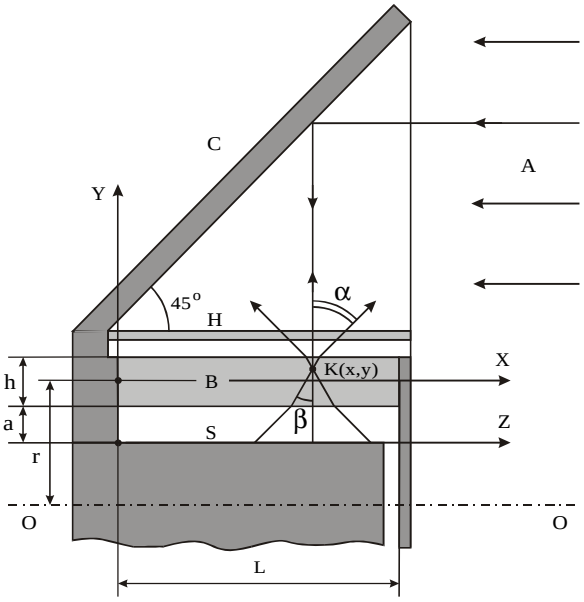

Figure 5. Panoramic optical tomograph.

photoemulsion *H*. Further the rays intersect the wall *B* of the cylindrical shell and, scattered by the immobile coaxial surface *S*, intersect the elements *B* and *H* at different angles. After two exposures the emulsion is developed and unrolled. Normal illumination of the hologram plane by a collimated reference beam produces an interference pattern that depends on view direction. The result of interference is determined by the change in the optical path caused by the change in the state f(x,y,w) of object elements passed by the beam. The function f(x,y,w) is determined by two factors: the change in the radial size *dh* of object element upon deformation and the change in its refractive index. For materials with low optical sensitivity and for small deformation gradient the second factor makes an insignificant contribution, that is why the interference fringes represent lines of equal thickness for each translucence direction. Let us restrict ourselves to consideration of translucences situated at axial cross sections of the shell. From these data we can reconstruct the function f(x,y) at each cross section using tomography.

A modification of the configuration in figure 5 allows us to find several other parameter fields of the state of the cylindrical shell:

1) If we cover the internal surface of shell *B* made of low optical sensitivity material with a light-scattering coating and fill in the space between *B* and *H* with immersion liquid, then it is possible to neglect the influence of the function f(x,y) on the optical path difference. As a result, the interference pattern allows to determine the displacement vector components of the points of the internal shell surface.

2) If it is necessary to find the refractive index distribution of an object in the stressed state, then in the configuration of figure 5, one must merely fill in the space between *B* and *S* as well between *B* and *H* with immersion liquid.

3) If we restrict ourselves to obtaining lines of equal width viewed in the radial direction, then it is possible to apply a photoemulsion to the external surface of the shell made of low optical sensitivity material, and a light-scattering coating on the internal surface.

In investigation of the deformed state of an optically transparent shell, the interference pattern for the configuration in figure 5 is projected onto the surface *S* with the coordinate grid. For some axial cross section of the shell we describe the optical path difference recorded on the interferogram by the function $\tilde{P}(z,a)$, where α is the view angle ($-\pi/2 < \alpha < \pi/2$). If there is no immersion, then from the geometry in figure 5, where the axis *X* is on the median surface of the shell, follows

$$z = x - y \cdot \mathrm{tg}\,\beta - T, \tag{8}$$

here $T = a \cdot \mathrm{tg}\alpha + h/2 \cdot \mathrm{tg}\beta$, β is the angular position of the beam in layer *B*, $\sin\alpha = n_o \cdot \sin\beta$. The value $\tilde{P}(z,a)$ consists of two components arising as the beam propagates through the object between the point of entrance to the photoemulsion and the point of exit from it. The first addend $P(z,b_s)$ collects the illuminating beam, the second one $P(z,b)$ – the scattered beam. As a result, the optical path collected by the scattered beam on the way from the point *z* of the surface *S* to the hologram *H* is expressed in terms of experimental data $P(z,b) = \tilde{P}(z,a) - \frac{1}{2} \cdot \tilde{P}(z,a_s)$, for figure 5 the angle $\alpha_s = 0$. While taking a photograph of the hologram at the angle α an interference pattern is recorded, that is why $\tilde{P}(z,a) = l \cdot m(z,a)$, where $m(z,\alpha)$ is the order of interference fringe viewed at the angle α at the point z of the surface *S*. Thus we find the integral projection

$$P(z,\beta) = l[m(z,\alpha) - (1/2) \cdot m(z,0)]. \tag{9}$$

Let the shell in the configuration of figure 5 be made of low optical sensitivity material, then the interference result is determined by the deformation value of the shell wall elements that the beam passed through

$$P(z,\beta) = n_o \cdot \int d(dl) = n_o \cdot \int e_l \cdot dl_o \,. \tag{10}$$

In the case of element deformation, we have $dl = dl_o (1 + \varepsilon_l)$, $dy = dy_o (1 + \varepsilon_r)$. The beam direction does not change, therefore, $dl / dy = dl_o / dy_o$ and $\varepsilon_l = \varepsilon_r$. The desired function denoted by $n_o \cdot \varepsilon_r = f(x,y)$, we have for the problem considered a definition of the integral projection

$$P(z,\beta) = \int f(x,y) \cdot dl_o \,, \tag{11}$$

where the element of beam path through the object $dl_o = \frac{dx}{\sin b} = \frac{dy}{\cos b}$. It is essential that for any direction shown in figure 5 the projection is defined by the same function f(x,y). That is why we can represent f(x,y) in terms of a set of its projections $P(z,\beta)$ by means of tomography.

Earlier the Radon transform was usually used for cross sections whose shape was nearly a circle, and the projections was taken to lines perpendicular to beams. In figure 5, the object cross section has the shape of a stretched rectangle, that is why in [3] the authors have developed the tomography methods as applied to a rectangular cross section and the coordinate object axes X, Y shown in figure, and the axis Z which is projected at an arbitrary angle. The Radon transform for this case leads to the following reconstruction formula:

$$f(x,y) = -\frac{1}{2p^2} \int_{-p/2}^{p/2} \frac{db}{\cos b} \int_{-\infty}^{+\infty} \frac{P(z,b)}{(z - z')^2} \cdot dz \,, \tag{12}$$

where $z' = x - y \cdot tgb - T$.

When using the Radon transform the filtered projection in the frequency region is proportional to $\hat{P}(w,b)\cdot|w|$ and projections with a low spatial frequency give a big error. Restricting ourselves to the low-frequency image component, we assume that the function of projections $\hat{P}(w,b)$ is unessential for $|w|>\Omega(b)$. We choose a frequency boundary independent of the illuminating beam directions and determined by the inverse value of the least distance *s* between them i.e. $\Omega(\beta) = (\pi / s)\cdot\cos\beta$. As a frequency window function, we choose the rectangular function

$$w_r(w,b)=\begin{cases}1 & for \quad |w|\le\Omega(b)\\ 0 & for \quad |w|>\Omega(b)\end{cases}. \tag{13}$$

In this case the approximate reconstruction has the form [3]

$$f_A(x,y) = -\frac{L}{2p^2}\int_{-\infty}^{\infty}\left(\frac{\partial^2 P(z,u)}{\partial z^2}\right)_{z=z}\cdot du\ , \tag{14}$$

where *L* is the length of the shell generatrix and u = tg β.

If a distribution under study has a low spatial frequency then the approximate reconstruction can be performed by means of the summarized image σ(x,y) corresponding to the method of classical tomography. For a two-dimensional cross section the reconstruction formula has the form [3]

$$s(x,y)=\frac{1}{ph}\int_{-p/2}^{+p/2}P(z,b)\cdot\cos b\cdot db\ . \tag{15}$$

Representing the functions σ(x,y) and f(x,y) in terms of their Fourier patterns we obtain the relationship

$$\hat{s}(w,b)=\frac{2\cos^2 b}{h\cdot|w|}\cdot\hat{f}(w,b)\ . \tag{16}$$

Thus, the summarized image reduces the object resolution for large spatial frequencies and large angles of illumination.

For experimental determination of the integrals of P(ζ,β) in equations (14), (15) the receipt and analysis methods on the basis of unrolled hologram are elaborated [4, 5]. We propose to use the converging cylindrical lens whose focus is aligned with the point under study of the virtual two-exposure image of the object. In this case all aspects of illumination over a wide range of view angles are taken into account.

REFERENCES

[1] L.A. Borynyak, E.A. Krasnopevtsev, Panoramic interferometry, *Optoelectronics, Instrumentation and Data Processing* **2** (1998) 13-25.
[2] Ch.M. Vest, *Holographic interferometry,* John Wiley & Sons, New York, 1979.
[3] E.A. Krasnopevtsev, L.A. Borynyak, Plane-parallel layer tomography, *Optoelectronics, Instrumentation and Data Processing* **4** (1999) 39-52.
[4] E.A. Krasnopevtsev, L.A. Borynyak, Panoramic interferometer with the maximal aperture, *Optoelectronics, Instrumentation and Data Processing* **4** (1999) 3-14.
[5] E. A. Krasnopevtsev, L.A. Borynyak, Panoramic interferometry (in Russian), Novosibirsk, 1999, 145 p.

AUTHORS: Ass. Prof. Dr. Eugene A. KRASNOPEVTSEV, Univ. Prof. Dr. Leonid A. BORYNYAK, Department of Physics, State Pedagogical University, Vilyuskaya 28, RUS-630126 Novosibirsk, Siberia, Russian Federation, Fax Int. +3832 68 1161, E-mail: spartak@online.sinor.ru